Geoderma 330 (2018) 41–51

Contents lists available at ScienceDirect

Geoderma

journal homepage: www.elsevier.com/locate/geoderma

Decoupling of topsoil and subsoil controls on organic matter dynamics in the Swiss Alps

Magalì Matteodo[a], Stephanie Grand[a,*,1], David Sebag[a,b,1], Mike C. Rowley[a], Pascal Vittoz[a], Eric P. Verrecchia[a]

[a] Institute of Earth Surface Dynamics (IDYST), Faculty of Geosciences and Environment (FGSE), University of Lausanne, 1015 Lausanne, Switzerland
[b] Normandie University, UNIROUEN, UNICAEN, CNRS, M2C, 76000 Rouen, France

ARTICLE INFO

Handling Editor: A.B. McBratney

Keywords:
Alpine environment
Organic matter stabilisation
Ecosystem properties
Litter decomposition
Rock-Eval pyrolysis
Thermal stability

ABSTRACT

Our understanding of mechanisms governing soil organic matter (OM) stability is evolving. It is gradually becoming accepted that soil OM stability is not primarily regulated by the molecular structure of plant inputs, but instead by the biotic and abiotic properties of the edaphic environment. Moreover, several experimental studies conducted in artificial systems have suggested that mechanisms regulating OM stability may differ with depth in the soil profile. Up to now however, there is very limited field-scale evidence regarding the hierarchy of controls on soil OM dynamics and their changes with soil depth.

In this study, we take advantage of the high heterogeneity of ecological conditions occurring in the alpine belt to identify the major determinants of OM dynamics and how their significance varies with depth in the soil profile. Aboveground litter, mineral topsoil, and subsoil samples originating from 46 soil profiles spanning a wide range of soil and vegetation types were analysed. We used Rock-Eval pyrolysis, a technique that investigates the thermal stability of OM, as an indicator of OM dynamics.

Our results show a clear divergence in predictors of OM thermal stability in the litter, topsoil, and subsoil layers. The composition of OM correlated with its thermal stability in the litter layer but not in mineral soil horizons, where the supply rate of fresh organic material and the physical and chemical characteristics of the pedogenic environment appeared important instead. This study offers direct confirmation that soil OM dynamics are influenced by different ecosystem properties in each soil layer. This has important implications for our understanding of carbon cycling in soils under a changing climate.

1. Introduction

Soil organic matter (OM) provides essential ecosystem services as it contributes to soil fertility, water quality and retention, biodiversity, resistance to soil erosion, and could play a fundamental role in the mitigation of climate change (Adhikari and Hartemink, 2016). Therefore, it is necessary to understand the mechanisms governing its stability, namely its preservation from mineralisation (Plante et al., 2011; Sollins et al., 1996; von Lützow et al., 2006) in order to maintain soil OM stocks and their associated functions. It was previously widely held that mineralisation rates of soil OM reflected the kinetics of enzymatic reactions and were consequently largely dependent on the intrinsic molecular composition of plant litter entering the soil system (Davidson and Janssens, 2006). This concept has been formalised under the term "selective degradation" (Sollins et al., 1996), and assumed that soil microorganisms preferentially decomposed the inherently labile components of OM, causing the accrual of recalcitrant components (Aber et al., 1990; Melillo et al., 1982). Recent studies have however questioned the idea that organic molecules could be inherently "stable" or "recalcitrant" (Lehmann and Kleber, 2015; Marschner et al., 2008) by showing that potentially persistent organic molecules, such as lignin, could be mineralised relatively quickly in soils (Gleixner et al., 1999, 2002; Heim and Schmidt, 2007). Contrarily, supposedly labile compounds, such as polysaccharides and proteins, can persist in soil for several decades, centuries or even millennia before being mineralised (Derrien et al., 2006; Gleixner et al., 1999, 2002). These long residence times can be in large part attributed to protection or stabilisation by soil minerals (Gleixner et al., 2002; Spielvogel et al., 2008). These recent findings have led to the proposal of a new paradigm, conceptualised by Schmidt et al. (2011). It suggests that selective degradation only plays an essential role in the initial stages of litter decomposition on the soil surface, while its importance becomes marginal when organic material

* Corresponding author.
E-mail address: stephanie.grand@unil.ch (S. Grand).
[1] Shared authorship: Stephanie Grand and David Sebag contributed equally to the work.

https://doi.org/10.1016/j.geoderma.2018.05.011
Received 27 November 2017; Received in revised form 7 May 2018; Accepted 9 May 2018
0016-7061/ © 2018 The Authors. Published by Elsevier B.V. This is an open access article under the CC BY-NC-ND license (http://creativecommons.org/licenses/BY-NC-ND/4.0/).

is incorporated into the mineral soil. In the mineral soil, OM decomposition rates would instead mainly be driven by its spatial accessibility to microorganisms, their enzymes and the necessary compounds of decomposition (mainly oxygen and moisture), and by the type and number of interactions established with mineral surfaces (Lehmann and Kleber, 2015; Schimel and Schaeffer, 2012; Sollins et al., 1996; von Lützow et al., 2006). OM stability in the mineral soil would thus be mainly governed by ecosystem properties such as climate, soil texture, mineralogy and geochemistry (see synthesis by Schmidt et al., 2011 and references therein).

Even though considerably high proportions (between 30 and 63%) of carbon (C) are stored in the subsoil, between 30 and 100 cm deep (Batjes, 1996), most of the studies on soil OM stabilisation mechanisms have focused on the topsoil (Rumpel and Kögel-Knabner, 2011). This may have resulted in a significant bias in our understanding of drivers of OM stability. Indeed, manipulative laboratory experiments suggest that factors controlling C dynamics in topsoil and subsoil may be substantially different. Fierer et al. (2003) and Salomé et al. (2010) incubated topsoil and subsoil material and found that water potential and supply of fresh organic material were important for surface horizons, while nutrient input, temperature, and the physical accessibility of organic substrates appeared as the main regulatory mechanisms of C mineralisation in the subsurface soil layers. Whether this divergence of controls on soil OM stability is operative under field conditions remains however difficult to evaluate.

Indeed, there is no universally recognised mean to assess soil OM stability. Many different fractionation techniques have been devised based on physical, chemical, or biological properties of OM (see Kögel-Knabner et al., 2008 for a review). Physical and chemical fractionation techniques separate soil OM into operationally-defined pools whose relevance to field-scale OM dynamics remains difficult to assess (Diochon et al., 2016). Investigations that consider the bulk sample without pre-treatment may allow for a more integrative assessment of OM stability. In this respect, biological mineralisation during long-term incubation experiments is generally favoured (Plante et al., 2011), but the inherent soil disturbance and the long durations of incubation required to be fully informative (up to several decades) represent an impediment. Thermal decomposition techniques offer a promising alternative to study soil OM stability. Results from thermal decomposition studies are consistent with those of incubation experiments (Plante et al., 2011) and some physical fractionation schemes (Gregorich et al., 2015; Saenger et al., 2015). The pertinence of thermal techniques is based on the assumption, validated by Plante et al. (2011), that the thermal stability of OM is related to its chemical properties or biological stability, as the activation energy required for thermal bond cleavage correlates to the chemical energy required for enzymatic cleavage (Kögel-Knabner et al., 2008). Schiedung et al. (2017) recently showed that thermal oxidation between 200 and 400 °C was a poor predictor of old (17 years or older) versus recent vegetation inputs. Pyrolysis techniques appear better suited to assess biological stability, as persistent OM tends to disintegrate at higher temperatures than labile OM (Barré et al., 2016). The Rock-Eval pyrolysis technique is now widely employed for routine analysis of OM in soil samples (see Sebag et al., 2016 for a review). This method quantifies total organic and inorganic C contents of a sample (either soil or litter) and provides a wide range of parameters that can be used to evaluate OM composition and its thermal stability. When compared to other methods used to quantify pools of recent or labile C (as assessed using ^{14}C dating, incubation and physical fractionation), Rock-Eval analysis performed most effectively (Soucémarianadin et al., 2018a; Vinduskova et al., 2015).

In this study, the thermal stability of OM, taken as an indicator of OM dynamics, was measured using Rock-Eval pyrolysis in litter (Oi horizon), topsoil mineral (A horizons), and subsoil mineral layers (including E, B, and C horizons) of 46 subalpine-alpine soil profiles. These soil profiles spanned eight types of vegetation communities and a wide range of soil pH and moisture conditions. The specific aims of this research were (1) to identify the major predictors of OM thermal stability and (2) to assess how their relative importance varied with soil depth. We hypothesised that there would be a clear shift in determinants of OM thermal stability between soil layers, with the influence of plant inputs being restricted to organic layers while the properties of the mineral phase would become prominent at depth.

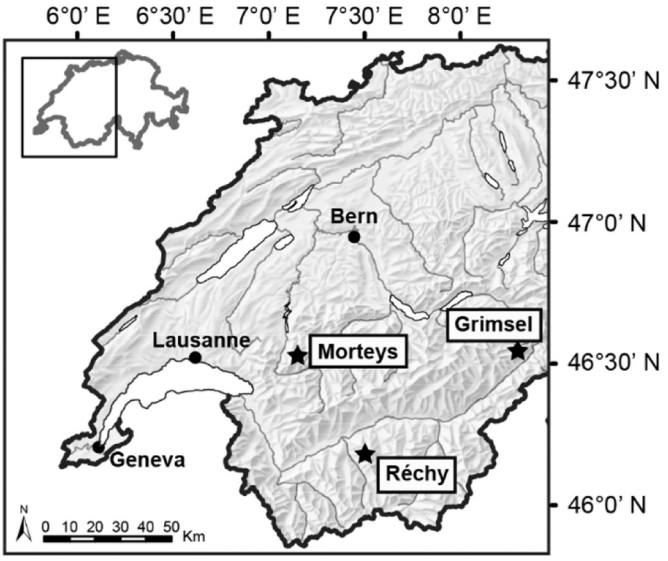

Fig. 1. Location of the three study sites (represented by a star) in Switzerland.

2. Methods

2.1. Sampling design

The 46 soil profiles were selected across three sites of northern and western central Alps in Switzerland (Fig. 1) differing in terms of lithology (Table 1). The Morteys site is underlain by compact limestone and calcareous surficial deposits, while the soil parent materials of the Grimsel site are mainly granite, gneiss, and granodiorite (Oberhänsli et al., 1988). The Réchy area is underlain by a variety of bedrock types including gneiss, mica schist, quartzite, calcschist, marble, and "cornieule" (a dolomite-gypsum greywacke). The three study sites were

Table 1
Characteristics of the study sites: coordinates, mean annual temperatures (MAT), mean annual precipitations (MAP), elevation ranges (with median between brackets), vegetation belt, vegetation types present, lithology, and number of soil profiles excavated at each study site. MAT and MAP are extrapolated according to Zimmermann and Kienast (1999) with a 25 m grid cell size.

	Morteys	Grimsel	Réchy
Latitude	46°32′N	46°32′N	46°10′N
Longitude	7°09′E	8°16′E	7°30′E
MAT [°C]	2.1	−0.44	−0.53
MAP [mm]	1650	2071	1480
Elevation [m]	1698–2232 (1884)	2310–2650 (2329)	2430–2697 (2573)
Vegetation belt	Upper subalpine	Lower alpine	Lower alpine
Vegetation types	Calcareous grasslands, subalpine pastures, calcareous snowbeds	Siliceous subalpine and alpine grasslands, typical snowbeds	Siliceous alpine grasslands, typical and wet snowbeds, windy ridges
Lithology	Limestone	Granite, gneiss, granodiorite	Gneiss, micaschists, quartzite, calcshists, marble, dolomite
No. of soil profiles	18	11	17

covered with glaciers during the last Pleistocene glaciation (Würm). The onset of the melting of the Rhône glacier in Switzerland is dated circa 21,000 years before present and continued to the oldest Dryas, around 16,000 years before present (Ivy-Ochs et al., 2004). This must be considered as the maximum soil age at our study sites. A variety of morphodynamic processes triggered the removal, transport, and accumulation of material during the Quaternary, leading to a complex mosaic of sediments of different ages (Baruck et al., 2016; Theurillat et al., 1998). Therefore, surficial deposits such as scree slope, moraine, and loess deposits are frequently found as soil parent materials. The climatic conditions differ slightly between the three study sites consistently with their biogeographic region and elevational belt. Due to its internal position in the Alps, the climate of the Réchy area tends towards drier continental conditions, while Morteys and Grimsel have a slightly more humid and oceanic climate (Table 1). All soil profiles are located above the present treeline. However, because of extensive grazing and deforestation in the Middle Age, the present treeline elevation is lower than it would be if driven purely by climatic influences (Favilli et al., 2010). We can estimate that the Morteys study site is located around the potential treeline (upper subalpine and lower alpine belt) and the Grimsel and Réchy sites slightly above it (lower alpine and alpine belt; Table 1).

Vascular plant species were exhaustively inventoried around each soil profile. Then, for simplification and standardisation purposes, the plant inventories with similar species composition and estimated cover were grouped by cluster analysis and, based on its dominant species, each group was associated to a specific plant community of the Swiss vegetation classification system (Delarze et al., 2015). This procedure identified a total of eight types of plant communities growing on the 46 soil profiles: (i) calcareous grasslands, (ii) subalpine pastures, (iii) windy ridges, (iv) calcareous snowbeds, (v) siliceous subalpine grasslands, (vi) siliceous alpine grasslands, (vii) typical (siliceous) snowbeds and (viii) wet snowbeds. Each vegetation type mirrors the ecological conditions where plants grow (Suppl. Table 1) and can therefore be considered as an “eco-unit” (Saenger et al., 2013). Vegetation in most plots was extensively grazed by cow, goat, or sheep for 2–4 months in summer, with the strongest grazing impact expected in subalpine pastures.

2.2. Soil description and analyses

Soil description was performed following the guidelines provided by the Food and Agriculture Organization of the United Nations (FAO, 2006). Depth, colour (according to the Munsell soil colour chart), relative abundance of calcium carbonate (established by 10% HCl test), structure, percentage of skeleton (rock fragments > 2 mm) and abundance of fine roots (< 2 mm in diameter) in each soil horizon were estimated in the field. Organic (Oi, Oe and Oa), mineral topsoil (A), and mineral subsoil horizons (E, B, and C) have been initially named according to Baize and Girard (2009) and then converted to the international FAO nomenclature (FAO, 2006). Classification of soils followed IUSS Working Group (2015) and that of humus forms followed Jabiol et al. (2013).

Samples were collected in a total of 231 horizons, including the organic horizons. Sampling occurred in early summer, within the three months following snow melt, irrespective of the vegetation type. Samples were dried at 45 °C. Mineral soil samples were then sieved at 2 mm (fine earth fraction) and a part of the sieved sample was crushed to powder in an agate mortar. The organic samples were ground to 0.12 mm mesh size with a pulveriser (14 Fritsch Tracomme AG). pH was measured in water (pH_{H2O}) with a lab pH meter (Metrohm SA) fitted with a double-junction combined glass electrode. The measurement was conducted in a suspension of fine earth in deionized water (1:2.5 soil water ratio) after 2 h of agitation. The texture of the fine earth fraction was assessed by laser diffraction. Prior to particle size analysis, calcium carbonate was removed by reaction with 10% HCl which was subsequently rinsed off until a pH > 6 was reached. The OM was then removed with 10–35% hydrogen peroxide (H_2O_2). During and after the OM digestion, excess acidity was neutralised with sodium hydroxide (NaOH) 0.1–0.5 M. Finally, soil mineral particles suspended in dilute Na-hexametaphosphate (40 g/L) were analysed in the diffractometer (Malvern™ Mastersizer 2000). Organic carbon and total nitrogen were measured on the dried crushed samples with a CHNS Elemental analyser (EA1108-Carlo Erba Instrument). Calcium carbonate was removed prior to analysis by addition of 10% HCl and subsequent rinsing. The C/N ratio was calculated for each organic and topsoil mineral layer. Unfortunately, N concentration in subsoil horizons was below the reliable quantification limit precluding the interpretation of C/N ratios there.

The total organic carbon (TOC) concentration and the OM properties of the 231 samples were obtained by thermal analysis performed with a Rock-Eval 6 Pyrolyser (Vinci Technologies). Twenty samples had TOC concentrations that were too low for reliable analysis (TOC < 0.2%) and/or abnormal pyrolysis curves (no smooth pyrograms in the S2, S3 or S4 regions indicative of measurement failure) and were deleted from the dataset; therefore 211 samples were retained for the analyses. Between 40 and 70 mg of dried crushed sample were pyrolysed in an inert N_2 atmosphere with increasing temperatures from 200 up to 650 °C with a heating rate of 25 °C/min. The residual sample was then oxidised under oxygenated atmosphere starting at a temperature of 400 increasing until 850 °C with the same heating rate.

The two phases of thermal decomposition released hydrocarbon compounds (HC), CO_2, and CO which were detected continuously. The sum of these C fractions (excluding the CO_2 released above 400 °C during N_2-pyrolysis and above 650 °C during oxidation, which corresponds to the mineral C) represents the TOC concentration (Lafargue et al., 1998). The TOC concentration correlated very well with the organic C concentration measured by elemental analysis ($r^2 = 0.98$, Suppl. Fig. 1). All element concentrations were calculated on an oven-dried soil basis. The hygroscopic moisture correction factor was determined by oven-drying dried crushed samples at 55 °C during 30 h for organic layers and 105 °C during 24 h for the other layers. The amount of HC released relative to TOC is called the Hydrogen Index (HI) and is considered proportional to the atomic H:C ratio in the sample. Similarly, the amount of CO_2 and CO released relative to TOC is called the Oxygen Index (OI) and it is considered proportional to the atomic O:C ratio. The HI and OI are regarded as proxies of the organic matter stoichiometry or composition (Carrie et al., 2012).

The amount of HC released during pyrolysis between 200 and 650 °C forms a bell curve called the S2 pyrogram. The shape of this pyrogram is sample-specific and is indicative of the thermal stability of organic molecules in the sample. The area under the S2 pyrogram was subdivided into four sections (A1, A2, A3 and A4) using temperature cut-offs frequently used in the literature (Sebag et al., 2016): 200–340 °C for A1, 340–400 °C for A2, 400–460 °C for A3 and 460–650 °C for A4. Thermally labile organic molecules release high quantities of HC during the early stage of the pyrolysis process (i.e. large A1 and A2 areas), while thermally stable organic molecules crack later (i.e. large A3 and A4 areas). On this basis, the thermal stability of each sample was represented by two indices previously proposed by Sebag et al. (2016): the R-Index representing thermally refractory OM [$R = (A3 + A4) / (A1 + A2 + A3 + A4)$], and the I-Index representing thermally labile OM [$I = \log_{10}(A1 + A2) / (A3)$]. These two indices are negatively correlated and only the R-Index was retained as an indicator of OM thermal stability in the present study (Suppl. Fig. 2).

The R-Index was preferred over other Rock-Eval parameters such as the OI, the HI, or temperatures at which 50% of C was evolved during the pyrolysis or oxidation phase (T50_HC_PYR or T50_CO2_OX, respectively), for the following reasons: (1) the OI and HI are more directly interpretable as indicators of OM stoichiometry than its stability; (2) T50_CO2_OX has been shown to correlate poorly with other measures of OM stability (Soucémarianadin et al., 2018a,b); and (3)

Table 2
Eighteen investigated potential drivers of OM thermal stability grouped under thematic categories. The scale (ordinal drivers), units (continuous ones), range, indications on whether they were included in the linear mixed models (LMM) specific to each soil horizon and their relative importance calculated with the IT-AIC analysis are given. Some drivers were excluded from the models to avoid collinearities or because they were not relevant in the soil horizon considered.

Category	Potential drivers of OM thermal stability	Remarks	Scale or unit	Range (median)	Relative importance in litter horizons	Relative importance in mineral topsoil	Relative importance in mineral subsoil
Site conditions	Mean summer temperature	Monthly average temperature for the period 1961–1990	°C	4.8–10.0 (6.6)	< 0.01	0.08	0.01
	Mean annual moisture Index	Precipitation - potential evapotranspiration (period 1961–1990)	mm	7147–15,108 (8658)	0.01	0.04	0.01
	North-South gradient	Equals to 0 - cosinus [radian (Aspect)]	–	From −1 (North) to 1 (South) (−0.03)	Collinear with solar radiation and Vegetation PC2 scores	< 0.03	< 0.01
	Mean summer solar radiation	Global potential shortwave radiation	KJ/day	17,080–28,902 (27030)	Collinear with North-South gradient and Vegetation PC2 scores	0.04	< 0.01
Vegetation type	Vegetation PC1 scores	Proportion of acidophilic species	Scores on the PC1 axis of a PCA based on species composition	From −0.3 to 0.2 (0.05)	< 0.01	Collinear with pH	0.49
	Vegetation PC2 scores	Proportion of hygrophilic species	Scores on the PC2 axis of a PCA based on species composition	From −0.2 to 0.2 (−0.01)	0.7	0.06	0.02
Soil properties	pH	For the litter layers, is the value of the first A horizon in the corresponding soil	–	3–7.9 (5.4)	Collinear with Vegetation PC1 scores	0.04	< 0.01
	Presence of carbonates	For the litter layers, it corresponds to the presence of carbonates within the soil profile	0 (absence), 1 (presence)	–	0.03	0.04	0.02
	Clay	Mineral particles < 0.002 mm diameter	% of fine earth fraction	1.1–48.5 (4.3)	Not relevant	Collinear with Sand	Collinear with Sand
	Silt	Mineral particles 0.002–0.063 mm diameter	% of fine earth fraction	31.7–87.1 (57.7)	Not relevant	0.06	0.47
	Sand	Mineral particles 0.063–2 mm diameter	% of fine earth fraction	3.2–65.4 (22.9)	Not relevant	0.04	0.51
Humus form properties	Humus Index	Modified from Ponge et al. (2002)	2 (Mesomull & Euanmoor), 3 (Oligomull), 4 (Dysmull), 5 (Hemimoder & Amphi), 7 (Dysmoder), 8 (Hemimor & Humimor)	2–8 (4)	0.02	0.03	< 0.01
	Waterlogged conditions	Presence of Anmoor humus forms (Jabiol et al., 2013)	0 (absence), 1 (presence)	–	0.02	0.05	0.01
	Rhizic humus form	Presence of > 25% of dead or living roots in the total volume of the O and A horizons combined (Jabiol et al., 2013)	0 (absence), 1 (presence)	–	Not relevant	< 0.03	0.01
OM properties	TOC	Total organic carbon concentration	% of fine earth fraction	0.45–59 (6.2)	< 0.01	1	< 0.01
	Hydrogen Index (HI)	Amount of hydrocarbons (HC) released relative to TOC	mg HC/g TOC	44.9–524.5 (267.3)	0.36	0.03	0.32
	Oxygen Index (OI)	Amount of CO and CO2 released relative to TOC	mg CO + CO2/g TOC	107.8–464.6 (216.2)	< 0.01	0.04	0.03
	C/N	Total carbon/total nitrogen	–	7.3–70.2 (14.7)	0.72	0.09	Not determined

T50_HC_PYR is by definition very close to and highly correlated with the R-Index, making its use redundant. Finally, Sebag et al. (2016) has shown that the R-Index is an appropriate proxy for OM dynamics during the decomposition process.

2.3. Potential drivers of OM thermal stability

A total of eighteen quantitative variables in five categories (site conditions, vegetation type, soil properties, humus forms and OM composition) were chosen for their potential impact on OM stability (Table 2). The mean air temperature in summer (June to September included), the average summer solar radiation and the mean annual moisture index (precipitation-evapotranspiration) were extrapolated for each soil location from the Swiss meteorological stations (www.meteoswiss.ch) according to Zimmermann and Kienast (1999). The aspect was measured in the field with a compass and then converted to a "North-South (NS) gradient" by the formula:

$$NS_{gradient} = 0 - \cos[radian(Aspect)].$$

The vegetation type was taken into account by performing a principle component analysis (PCA) based on the species composition and cover (after Hellinger transformation; see Legendre and Gallagher, 2001) recorded at each study point. Scores on the first two axes (Suppl. Fig. 3) were retained for subsequent analyses. The two resulting variables were respectively called Vegetation PC1 scores and Vegetation PC2 scores. To facilitate interpretation of these principal components, Landolt ecological indicator values (Landolt et al., 2010) expressing plant-specific requirements for soil pH (R) and moisture (F) were associated to each plant species of the dataset. A global indicator values for each plant inventory was calculated with the species cover as a weight. Finally, the Pearson correlation coefficient between the mean indicator values and the PC1 and PC2 scores of each plant inventory were calculated. Landolt's R value, corresponding to an increasing preference for alkaline soils, correlated strongly and negatively with Vegetation PC1 scores (Pearson's $r = -0.88$, 95% confidence interval = $-0.93 < r < -0.80$). Landolt's F value, corresponding to increasing requirement for soil moisture, was positively correlated with Vegetation PC2 scores ($r = 0.54$, $-0.30 < r < -0.72$). Vegetation PC1 scores were thus mainly related to the proportion of acidophilic species, and separated plant communities typically associated with calcareous versus siliceous substrates. Instead, Vegetation PC2 scores reflected in part the contribution of hygrophilic species and distinguished grasslands from snowbeds.

Soil properties included pH_{H2O}, clay (< 2 µm), silt (2–63 µm) and sand (63–2000 µm) percentages and the occurrence of carbonate (presence/absence of 10% HCl reaction). The humus form, i.e. the sequence of organic and underlying topsoil mineral horizons, was selected to represent the integrated effects of plant and decomposer communities. In this study, the humus form was represented by the Humus Index (modified after Ponge et al., 2002) spanning from 2 (MULL) to 8 (MOR). The presence of waterlogged and rhizic conditions (binary variables) was assigned, respectively, to the histic Anmoor humus forms (Jabiol et al., 2013) and to humus forms having > 25% of dead or living roots in the total volume (Jabiol et al., 2013). The OM properties consisted in the TOC concentration and three indices of OM composition: the HI and OI from Rock-Eval pyrolysis and the C/N ratio.

Finally, we also investigated the relation between class variables and OM thermal stability. Class variables included the lithological origin of soil's parent material, pedogenic environments and horizon type. Soil's parental lithology was assigned using our field observations as well as existing geological and geomorphological maps (www.swisstopo.admin.ch). We assigned three categories of parental lithologies: (1) a "calcareous" category referring to limestones, calcareous sandstones, marbles, and surficial deposits (screes and moraines) derived almost exclusively from these materials; (2) a "mixed" category containing surficial deposits of mixed origin (sedimentary, metamorphic, and igneous components); and (3) a "Si-rich" category containing granite, gneiss, quartzite, and surficial deposits derived almost exclusively from these materials. Pedogenic environments and horizon types were assigned on the basis of field description and results of soil lab analyses. We recognised four main types of pedogenic environments based on the degree of soil development and organic matter mobility. First, weakly differentiated solums (Cambisols, Leptosols, Regosols, Gleysols, Stagnosols) were set apart from podzolic solums with strong horizon differentiation. Secondly, within weakly-differentiated solums, we set apart circumneutral (subsoil pH > 6) from acid (subsoil pH < 5.6) profiles, hypothesising a difference in organic matter dynamics due to charge, dispersion and opportunity for mineral-association (Rowley et al., 2018). Likewise, we set apart Humic Podzols characterized by a strong accumulation of organic compounds to the subsoil, from Ferric Podzols where subsoil accumulation is dominated by Fe and Al compounds. We grouped horizon types following the same guiding principles into four general classes. The "podzolic" class included podzolic E, humic B (Bh), ferric B (Bs) and podzolic C horizons. The "weakly differentiated" class included Bsi (siliceous, low Ca saturation), Bci (absence of Ca-carbonate but high Ca saturation), Bca (presence of calcium carbonate) and C horizons. The next class was associated with soils with expressed redoximorphic features and included Bg (stagnic conditions) and Br (strong reducing conditions) horizons. The last class referred to buried A horizons (FAO, 2006).

2.4. Statistical analysis

The litter (Oi horizon), topsoil mineral (A horizon) and subsoil mineral layers (E, B and C horizons) were considered separately in the statistical analyses. The Oe and Oa horizons were excluded because of their low occurrence in the data set (respectively 6 and 4% of the samples). An information theoretic framework based on the Aikaike's information criterion (IT-AIC, Burnham and Anderson, 2002) was employed in order to find the dominant factors influencing OM thermal stability in each layer. Contrary to the traditional null hypothesis testing (Anderson et al., 2000), the IT-AIC approach fundamentally explores range of alternative fits (a "model set") potentially associated to a certain phenomenon and highlights the strongest associations worthy of further investigations (Symonds and Moussall, 2011). In the present study, a set of linear mixed-effects models (LMM) was built with the R-Index as dependent variable and the potential drivers of Table 2 as independent variables, standardised to a mean of 0 and a standard deviation of 0.5 according to Gelman (2008). The study sites and mean horizon depth were set as random effects in order to discount their potential influence on OM thermal stability. The independent variables (predictors) to be included in the models were scrutinised in order to avoid problematic collinearities. For each layer, groups of variables having a Spearman's rank correlation coefficient higher than 0.7 were identified, and the strongest predictor was retained. We also checked that the choice of the alternative variable did not affect ranking of the other predictors. The model set was composed of every possible combination of the variables, including an intercept-only model. According to Harrell (2001), the number of predictor variables simultaneously considered in each model should not exceed 1/10 of the sample size to avoid over-parameterisation. As the sample size of the litter layers was 33, the maximal number of predictors simultaneously considered in each model was set to 3. The same maximum number of predictors was used for mineral topsoil and subsoil horizons, although the number of samples was higher (77 and 69, respectively), to ensure that each analysis operated under similar constraints. The models composing the set were then compared and ranked by their AIC_C (modified version of AIC recommended for small sample sizes; $AICc = AIC + (2k^2 + 2k) / (n - k - 1)$, with n = sample size and k = number of estimated parameters). The approximation power of each model was expressed as the difference (ΔAIC_C) between the AIC_C of the best model (the lowest AIC_C value) and the AIC_C value for each of the other models. The ΔAIC_C was

then used to calculate the Aikaike weight (w_i) representing, for a given model, the probability to be the best approximating model within the model set. In this study, a "top model set" was created by subsetting the models that had a cumulative Aikaike weight of ≤ 0.95. Then, within the top model set, the relative importance of each variable was calculated by summing the Aikaike weights of the model(s) containing that variable. The factors having the strongest effect on the response variable were those with the highest summed Aikaike weights, i.e. having a relative importance tending towards 1 (Burnham and Anderson, 2002).

The relationship between the response variable (R-Index) and the factors having the highest relative importance was measured by the Pearson correlation coefficient and its 95% confidence intervals. The lower the confidence interval width, the higher the probability of the Pearson correlation coefficient to correctly reflect population correlation.

Finally, the role of class variables (soil parent material, pedogenic process, horizon type) on OM thermal stability, which could not be evaluated through the IT-AIC analysis, was investigated using a one-way analysis of variance (ANOVA). Diagnostics for assumptions of normality, homoscedasticity, and goodness-of-fit were performed on residual plots. For significant effects, pairwise *t*-tests without adjustment for multiple inferences (Webster, 2007) were performed to identify significant differences between R-Index means. The alpha level for significance was set to $\alpha = 0.05$ for all tests.

3. Results

3.1. Thermal stability of the OM increases with depth in the soil profile

The R-Index, i.e. the proportion of refractory compounds in the pyrolysed OM, increased with depth in the soil profile, from litter to topsoil and subsoil mineral layers. In contrast, the I-index, a proxy for preservation thermally labile, decreased with depth (Suppl. Fig. 2). This progressive increase in OM thermal stability with depth was observed in each of the eight vegetation types.

3.2. Factors influencing OM thermal stability in the litter layer

According to the IT-AIC analysis, OM thermal stability in the litter layer was mainly related to the OM stoichiometry (C/N ratio and Hydrogen Index, HI) and the proportion of hygrophilic species (Vegetation PC2 scores; Fig. 2). The R-Index correlated negatively with the C/N ratio ($r = -0.72$, $-0.85 < r < -0.50$) and positively with Vegetation PC2 scores ($r = 0.79$, $0.61 < r < 0.89$). The Hydrogen Index (HI), representing the proportion of hydrogen (H) relative to C atoms in OM, ranked as the third most important factor and was negatively related to the R-Index ($r = -0.65$, $-0.81 < r < -0.39$; Suppl. Fig. 4). The litter from snowbeds showed the lowest C/N ratios and HI values but the highest OM thermal stability.

3.3. Factors influencing OM thermal stability in the mineral topsoil

In the topsoil (A horizons), the thermal stability of the OM was predominantly related to its concentration (Fig. 3). The correlation between the R-Index and total organic C (TOC) concentration was negative and relatively weak ($r = -0.53$, $-0.67 < r < -0.34$). When the topsoil was OM-rich (TOC > 15%), the OM thermal stability was comparatively low. In some cases, these OM-rich A horizons were water-saturated for more than six months per year and displayed a hydromorphic humus type (classified as Anmoor; Jabiol et al., 2013). In others cases, the OM-rich A horizons had a large proportion of roots, and finally some of them presented a certain amount of fragmented litter homogeneously mixed with the fine earth fraction, likely resulting from bioturbation.

It should be noted that 28 of the 46 soil profiles presented several A horizons. In these cases, the OM of the most surficial A horizon systematically had a lower thermal stability than the underlying one (Suppl. Fig. 5), indicating increasing proportions of thermally stable OM with depth. To further investigate the hierarchy of predictors of OM thermal stability, we repeated the analysis with depth included as a fixed effect rather than a random one. This allowed us to compare the effectiveness of explanatory variables compared to that of depth. The main predictor of OM thermal stability remained the TOC concentration and was very closely followed by depth (Suppl. Fig. 6). This means that the predictive power of TOC concentration is of the same order as that of depth. The correlation between TOC concentration and depth was relatively weak ($r = -0.48$).

3.4. Factors influencing OM thermal stability in the mineral subsoil

The OM thermal stability in the subsoil was negatively related to the sand content and positively to the proportion of acidophilic species

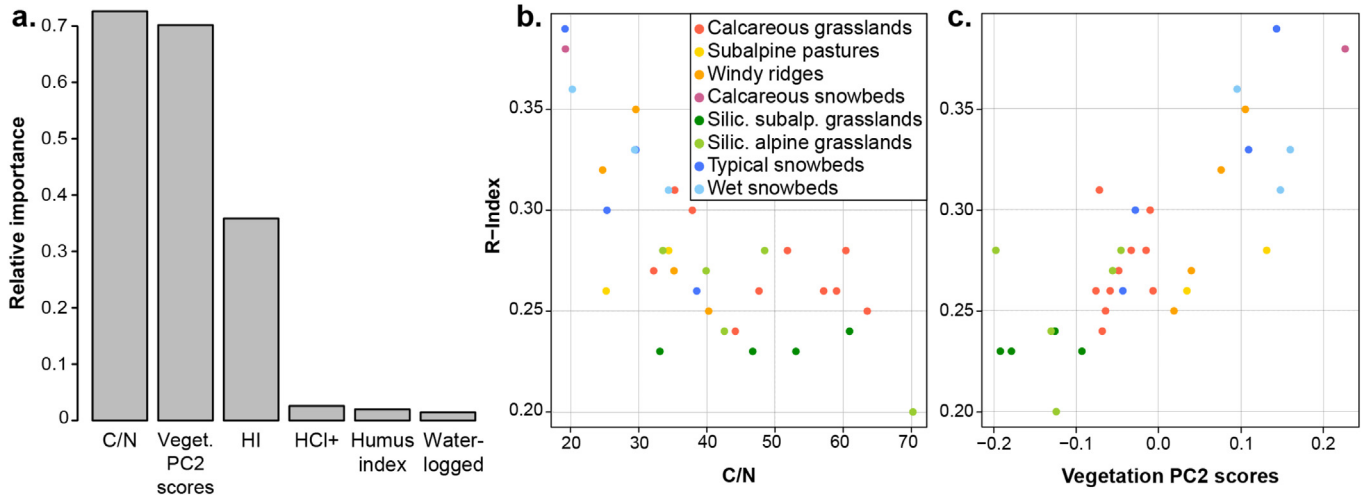

Fig. 2. Predictors of OM thermal stability in the litter layer. (a) The six main explanatory variables influencing the R-Index in the litter layers, ranked according to their relative importance. "Veget. PC2 scores": scores on the 2nd axis of a principle component analysis based on vegetation composition and cover, corresponding to a gradient of increasing contribution of hygrophilic species; "HI": Hydrogen Index; "HCl+": visible effervescence upon strong acid addition due to the presence of carbonate in the soil; (b and c) R-Index values plotted against the two most important predictors, C/N and Vegetation PC2 scores. Colours represent the eight plant communities. "Silic.": siliceous. "subalp.": subalpine.

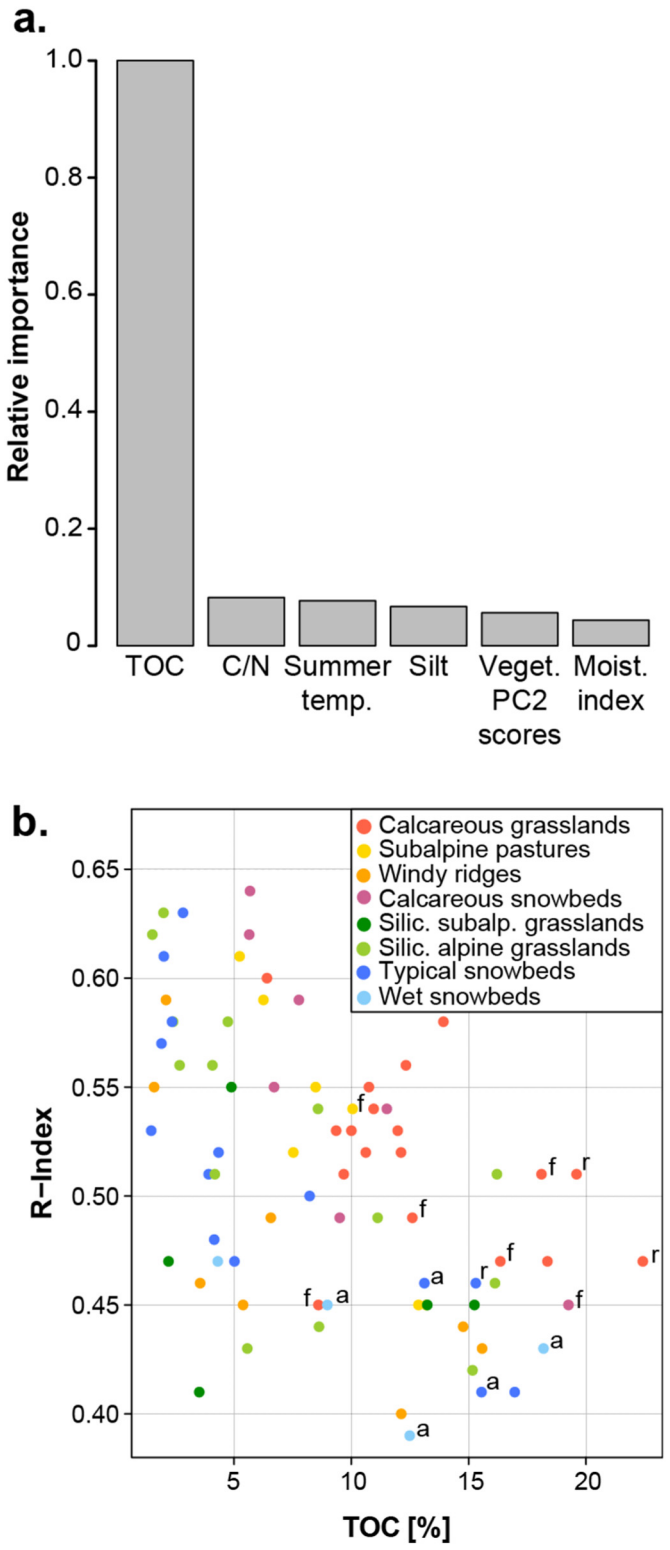

Fig. 3. Predictors of OM thermal stability in the mineral topsoil. (a) The six main explanatory variables influencing the R-Index in the topsoil, ranked by their relative importance. "TOC": total organic C concentration; "Summer temp.": mean summer temperature; "Silt": % of mineral particles having a diameter between 0.002 and 0.063 mm; "Moist. Index": mean annual moisture index (precipitation – potential evapotranspiration) (b) R-Index values plotted against the organic C concentration (TOC %). Colours represent the eight plant communities, while letters represent peculiarities of the A horizon. "a": hydromorphic A (Anmoor in Jabiol et al., 2013); "r": rhizic humus form, presence of > 25% of dead and living roots in the total volume of O and A horizons combined (Jabiol et al., 2013); "f": fragmented litter homogeneously mixed with fine earth fraction.

(Vegetation PC1 scores; Fig. 4b and c). The correlation remained weak in both cases ($r = -0.33$, $-0.52 < r < -0.10$ and $r = 0.25$, $0.01 < r < 0.46$, respectively). Silt and HI ranked respectively as third and fourth most important predictors (Suppl. Fig. 7). For comparison, the predictive power of these factors greatly exceeded that of horizon depth when included as a fixed effect (Suppl. Fig. 8). The correlation between the R-Index and texture variables (sand and silt proportion) was mainly driven by three eluvial (E) horizons, which were particularly sandy. If these three samples were removed from the analysis, the importance of texture was reduced and Vegetation PC1 scores became the most important predictor, followed by sand and silt proportions (not shown).

This study took place in the alpine environment, with little human activity, and as such the respective vegetation type reflected each site's ecological conditions (Vonlanthen et al., 2006; Grand et al., 2016). Vegetation PC1 scores represented a gradient of plant community preference for alkaline soils (Landolt et al., 2010) and could thus be considered as a proxy for soil geochemistry, as determined by the nature of the geological substrate and pedogenic environment. The nature of the geological substrate indeed explained 74% of the variance in Vegetation PC1, while the pedogenic environment explained 62% of the variance in Vegetation PC1 (Suppl. Fig. 9). This interpretation is confirmed by the correlation between Vegetation PC1 and soil pH (Suppl. Fig. 10).

Soil geochemistry was best represented by class variables that were not suited to the IT-AIC analysis. We therefore conducted a separate analysis of variance to test the effect of geological and soil classes on the R-Index of subsoil horizons (Suppl. Fig. 11). Geological classes explained 19% of the variance in the R-Index, with samples associated with Si-rich lithologies having a significantly higher R-Index than samples associated with calcareous or mixed lithologies. Soil classes explained 26% of the variance in the R-Index, with ferric podzols having a significantly higher R-Index than other soils.

Moreover, thermal stability of subsoil layers varied according to the type of horizon considered (Fig. 4d) and the pattern was not reducible to horizon depth, as could be observed in the topsoil (Suppl. Fig. 5). E horizons showed the lowest R-Index values, reaching the same range of thermal stability displayed by A horizons (Fig. 3), while buried A horizons (IIA; corresponding to fossil soils) showed among the highest R-Index values. B and C horizons showed intermediate values. Significant differences could be noted according to the different pedogenic processes at work: in podzolic profiles, OM thermal stability increased dramatically from eluvial (E) to illuvial horizons and was highest in horizons dominated by the accumulation of sesquioxides (E ~ Bh < Bs ~ podzolic C). In weakly developed soils, OM thermal stability increased slightly from carbonate-rich to siliceous horizons (Bca < Bsi). In redoximorphic horizons, OM thermal stability was generally variable and within range of other acid B and C horizons. Overall, the horizon type and associated pedogenic process had detectable effects on the OM thermal stability of the mineral subsoil layers.

4. Discussion

Due to its complex topography, geology, and geomorphology, the Alpine environment generates steep natural gradients of vegetation, soil moisture, texture, and geochemistry over very short spatial scales. This natural variability was used to explore controls on OM thermal stability. Study sites displayed a small climatic gradient (restricted region in the Alps and limited elevation range). Accordingly, climate-related variables (mean summer temperature, moisture index, and solar irradiance) were not found to be important predictors of OM thermal stability in the data set, likely due to the comparatively small range of variation in these factors. Furthermore, anthropogenic impact on these soils were not believed to have exerted a paramount influence since study sites have never been ploughed, but have been used for extensive pasture, largely replacing natural grazing by deer, gams or ibex.

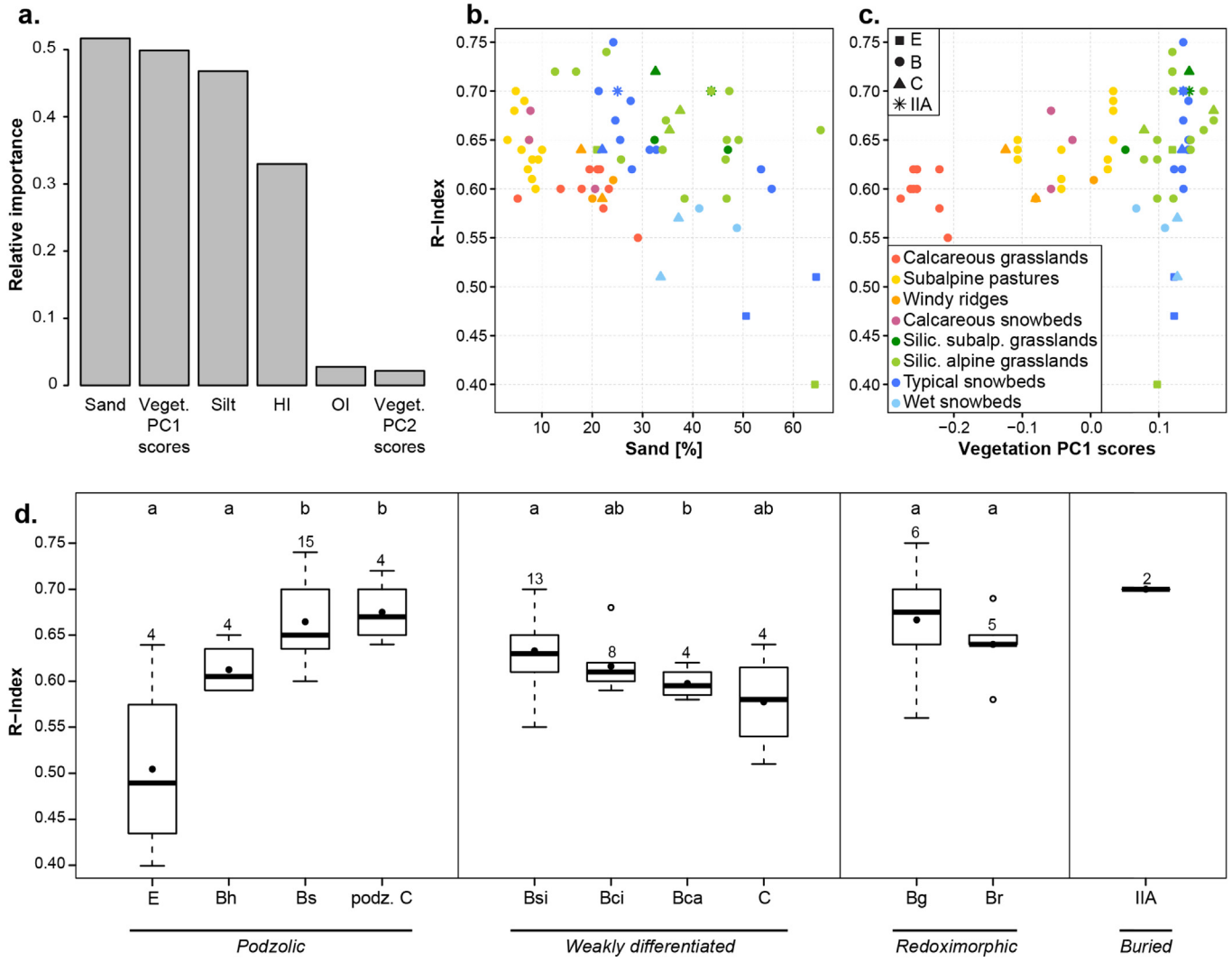

Fig. 4. Predictors of OM thermal stability in the subsoil. (a) The six main explanatory variables influencing the R-Index in the subsoil, ranked by their relative importance. "Veget. PC1 scores": scores on the 1st axis of a principle component analysis based on vegetation composition and cover, corresponding to a shift from calcophilic to acidophilic species. (b and c) R-Index values plotted against the two most important variables, Sand and Vegetation PC1 scores. Colours represent the eight plant communities and symbols represent the horizon categories. (d) Boxplots of R-Index by mineral horizon types. The first four horizon types represent the podzolic soil sequence, including "E" (eluvial horizon); "Bh" (illuvial accumulation of organic matter); "Bs" (illuvial accumulation of sesquioxides); "podzolic C" (C horizon underlying a podzolic profile). The next four horizon types are found in weakly-developed solums, such as Cambisols, Leptosols, and Regosols, and include: "Bsi" (siliceous, low Ca saturation); "Bci" (absence of Ca-carbonate but high Ca saturation); "Bca" (presence of Ca carbonate); "C" (subsoil horizon weakly affected by pedogenic processes). The next two horizon types are found in soils with expressed redoximorphic features and include "Bg" (stagnic conditions) and "Br" (strong reducing conditions) horizons. The last class "IIA" refers to buried A horizons (FAO, 2006). Black dots represent the mean values, the black line is the median, and boxes are limited by 1st and 3rd quartiles. Numbers of observations are indicated above boxplots. Letters above boxplots indicate significant differences (p-value < 0.05) calculated by pairwise *t*-tests conducted within broad classes of horizon types.

We used the Rock-Eval R-Index, which gives a snapshot of the proportion of thermally refractory compounds found within the OM, as a proxy for organic matter dynamics, broadly understood as processes leading to changes in OM properties. The use of Rock-Eval pyrolysis allowed us to evaluate OM properties similarly across all soil layers without applying any pre-treatment, and thus eliminated the risk of creating experimental artefacts. As expected from results of other studies employing Rock-Eval analysis (Sebag et al., 2016 and references therein), we found that the contribution from thermally stable OM progressively increased with depth in the soil profile (Suppl. Fig. 1). This is in accordance with the generally accepted idea that in the absence of perturbations, soil OM stability and residence time tend to increase with depth (van der Voort et al., 2016). However, the R-Index of subsoil horizons retained significant variability (Fig. 4d). Moreover, differences in subsoil horizons could not be predicted from differences observed in the litter layer or even the A horizon (Suppl. Fig. 12). As an example, wet snowbeds had relatively high R-Index values in the litter layer, but showed the lowest values in mineral horizons; siliceous subalpine grasslands had among the lowest R-Index values in the litter and topsoil horizons, but they showed the highest values in the subsoil (Suppl. Fig. 13). This indicated that soil OM dynamics, as represented by changes in OM thermal properties, followed diverging trajectories with depth in different edaphic environments. In the next sections, we will explore the factors correlated with OM thermal stability in each major soil layer (litter, topsoil, and subsoil) and their significance.

In the litter layer, the thermal stability of OM varied according to its stoichiometry (C/N and Hydrogen Index – HI) and to the plant community producing it (Vegetation PC2 scores). Differences in the C/N and HI in the litter layer may arise both from the initial biochemical OM composition and from the litter mineralisation degree. Variations in C/N ratios were driven by differences in N rather than organic C concentration (Suppl. Fig. 14). Plants with efficient N uptake mediated by

mycorrhizal fungi or N-fixing capacity may produce N-enriched litter. These characteristics are present in some vascular plant and moss species of snowbeds (Woolgrove and Woodin, 1996; Mullen et al., 1998), which showed the lowest C/N ratio and highest R-Index values (Suppl. Figs. 13 & 14). The process might be further enhanced by N accumulation in the snowpack, acting as a scavenger of air pollution (Knutson et al., 1976). On the other hand, N accumulation (Aber and Melillo, 1982; Manzoni et al., 2008) and OM dehydrogenisation (Barré et al., 2016; Sebag et al., 2016) typically occur during decomposition. Low C/N and HI values may be used as an indicator of the mineralisation degree (Grand and Lavkulich, 2012). The inverse relation between the litter thermal stability and the C/N and HI values may reflect the fact that a more thermally recalcitrant OM is produced as decomposition proceeds. In this study, litter was collected in summer and thus essentially consisted in material that had senesced nearly a year ago (during the previous fall). The concomitant increase in thermal stability and the proportion of hygrophilic species could also indicate that longer periods of snow cover favour decomposition (Baptist et al., 2010; Hobbie and Chapin, 1996) and selectively preserve thermally resistant components (Sebag et al., 2016). Overall, the increase in the R-Index, concomitant with the increase in N and decrease in H content, corroborates the common observation that OM properties in the litter layer simply reflect the quality of plant inputs and the extent of decomposition.

In the A horizons, the main predictor of OM thermal stability, among the 18 factors under study, was the concentration of soil C (Fig. 3), which is in turn related to the balance between mechanisms governing the fresh OM inputs and those controlling its mineralisation or deep translocation. The predictive power of organic C concentration on OM thermal stability was surprisingly large, matching that of depth (Suppl. Fig. 6). The main split seemed to occur at an organic C concentration of about 15%. Below this threshold, the R-Index of OM was highly variable while above this threshold, the R-Index was consistently low (Fig. 3). Many of the organic C rich samples had unusually large amounts of roots or visible litter fragments (indicative of active bioturbation delivering plant material to the mineral soil). Other displayed traces of hydromorphy. Our sample set, restricted to a semi-natural environment, thus contained a significant proportion of samples with a high concentration of fresh OM displaying a thermally labile signature. In the same way, Sebag et al. (2006) observed lower R-indices in soil layers under dense plant cover (large inputs) when compared to sparse vegetation (low inputs).

These findings indicate that the thermal signature of OM in the A horizon was related to physical processes of OM delivery into the mineral soil. The thermally labile signature of the OM-rich samples could be due to several processes. Roots or litter-rich samples probably record a kinetic phenomenon in which the thermal signature of the OM is constantly 'refreshed' by abundant new inputs. A decline in enzymatic efficiency at high substrate availability might play a role (Schimel and Weintraub, 2003). For hydromorphic samples, it is well-known that oxygen limitation can initiate a transition towards alternative respiratory pathways that are less energy efficient, and thus a reduction in decomposition (Schlesinger and Bernhardt, 2013). Furthermore, at high organic loadings, the potential for OM stabilisation by interactions with mineral surfaces decreases (Six et al., 2002). Organic-rich samples are thus likely dominated by light particulate OM fractions, which generally represents a thermally labile OM pool (Saenger et al., 2015; Soucémarianadin et al., 2018a). Overall, our results indicate that thermal stability of topsoil OM is controlled by pedogenic processes rather than OM composition or stoichiometry.

In subsoil mineral layers, OM thermal stability was mainly related to texture and Vegetation PC1. However, the predictive power of these factors was modest, indicating that a major part of OM thermal stability in the subsoil remained unexplained by the present dataset. Vegetation PC1 represented a gradient of calcophilic to acidophilic species and could thus be interpreted as a proxy for soil geochemistry (Suppl. Figs. 9 & 10). Recognising the indirectness in inferring soil geochemistry from plant communities, we performed an additional analysis of variance which confirmed that geological and pedogenic classes had a strong explanatory power on R-Index variations in the subsoil (Suppl. Fig. 11). Variance explained by geology (19%) and soil (26%) classes were actually larger than that explained by Vegetation PC1 (6%). This result concurs with a recent study of instantaneous OM mineralisation rates (represented by soil-surface efflux, also known as soil respiration) in mountain soils, which found that 17% of the variation in whole-soil respiration could be explained by soil classes (Grand et al., 2016). Soucémarianadin et al. (2018b) suggested that soil class could constitute an integrated parameter capturing important differences in OM turnover; yet, pedogenic parameters are conspicuously absent from most models of soil OM cycling. Interestingly, we found that texture (% sand, silt, or clay) was only slightly related to the R-Index of OM in subsoil layers once special pedogenic dynamics were accounted for, such as that associated with the E horizons of podzols. This finding is consistent with the results of a recent large meta-analysis (Rasmussen et al., 2018) which showed that chemical and mineralogical parameters far exceeded the predictive power of clay on soil OM stabilisation.

Moreover, significant differences in OM thermal stability were observed between subsoil horizon types (Fig. 4d), which could not be simply explained by an increase in the R-Index with depth. We instead hypothesise that various stabilisation mechanisms, associated to specific pedogenic processes, could be responsible for the observed variations. According to von Lützow et al. (2008), stabilisation mechanisms are indeed horizon-specific in Podzols. The potential for organo-mineral interactions is thought to be low in eluvial horizons, where long-chain alkyl structures could accumulate (Rumpel et al., 2004), perhaps as a result of hydrophobic separation from decomposers. Complexation of organics with monomeric Al and Fe has been proposed as the main stabilisation mechanism in Bh horizons while Bs and podzolic C horizons typically contain highly oxidised OM stabilised by organo-mineral interactions, such as ligand-exchange (Rumpel et al., 2004; von Lützow et al., 2008). Interestingly, OM thermal stability in Podzol mineral layers measured in this study increased in the order E ~ Bh < Bs layers (Fig. 4d). In accordance with the conceptual model outlined by Rumpel et al. (2004), a possible interpretation is that E horizons contained mostly C and H-rich, thermally unstable moieties (Suppl. Fig. 15), while Bh and Bs horizon were enriched in partially dehydrogenated, thermally stable molecules. Moreover, our results might suggest that OM interaction with metals, believed to dominate in Bh horizons, have a weaker effect on OM properties than interactions with poorly crystalline oxides and aluminosilicates, expected in Bs horizons.

A potential stabilisation mediated by Ca was less apparent in our dataset (Fig. 4d), but OM present in Ca-rich horizons (Bca) was more thermally labile, and thus perhaps less processed, than the OM present in Ca-poor horizons (Bsi). This may indicate that aggregation and protection of some thermally labile OM by occlusion within aggregates were more pronounced in Ca-rich horizons (Rowley et al., 2018). Moreover, plant roots were visibly more abundant in the calcareous subsoils than in their siliceous counterparts, and their turnover could partly explain the large concentration of labile OM in Ca-rich B horizons. Redoximorphic processes (Bg and Br horizons) were not associated with a specific OM thermal signature, perhaps due to the typically seasonal nature of waterlogging in alpine soils. Overall, our result supports a dominant role of the geochemical properties of the mineral matrix on OM dynamics in the subsoil. Further investigation is needed to establish whether the thermal resistance measured by Rock-Eval pyrolysis is indeed reflective of the type of organo-mineral association involved.

As previously proposed by Salomé et al. (2010), this study confirmed a substantial decoupling between organic, topsoil, and subsoil mineral horizons in terms of factors influencing OM dynamics, as represented by its thermal stability. This study was consistent with the repeated findings of litter bag experiments (e.g. Preston et al., 2009)

showing that the intrinsic properties of OM (litter source) and its selective degradation play a role at the beginning of the OM decomposition continuum (Lehmann and Kleber, 2015), in the litter layer, before any pervasive opportunity for interaction with the mineral matrix. Contrarily, in the topsoil and subsoil mineral layers, our data showed that OM dynamics were influenced by the pedogenic environment, rather than being an intrinsic property driven by its initial composition. In these layers, the vegetation type played an indirect role on soil OM thermal stability by determining the rate of plant inputs entering the soil system and its vertical distribution along the soil profile (Jobbagy and Jackson, 2000), rather than by determining its quality. As observed in many studies (Kögel-Knabner et al., 2008; Rumpel et al., 2002), soil OM dynamics in subsoil horizons seemed to be driven by the types and intensity of organo-mineral interactions and physical protection from decomposers. Consistently with our initial hypothesis, our study thus evidenced a clear shift in determinants of OM dynamics between soil horizons, with the influence of the litter source and OM stoichiometry seeming preeminent in organic layers and properties of the mineral phase rising to the forefront in the subsoil.

It should be noted that the 18 factors explored in this study were not exhaustive. In particular, we expect that measures of the molecular composition of plant materials and composition of the decomposer community could yield important further insights into OM dynamics in the litter layer. In the mineral soil, we used proxies for soil mineralogy and geochemistry (lithological origin of soil's parent material, pedogenesis, presence of acidophilic/calcophilic species). We expect that detailed measures of mineralogical and geochemical parameters (e.g., specific surface area, clay mineralogy, oxide content and crystallinity, carbonate content and crystallinity, base saturation, etc.) would provide more details on processes governing OM dynamics in the mineral soil. Furthermore, our study was restricted to semi-natural grasslands of the alpine and subalpine belts. This area is characterized by uncultivated, young soils with relatively small amounts of secondary minerals. Other studies in areas with diverse land uses and more pedogenetically advanced profiles are needed to extend these results beyond mountain regions.

It is generally thought that global warming will increase soil organic C mineralisation (Leifeld et al., 2009; Schimel, 1995). The present study suggests that the effects of climate change will not be reducible to changes in OM mineralisation rates as a result of the temperature-dependency of enzymatic degradation (Q10-effects); indeed, pure Q10-effects are likely to be of minor importance when compared to broader ecosystem consequences. Our study suggests that shifts in plant communities and in pedogenic trajectories could result in drastically altered OM dynamics. This constitutes a critical research gap which undermines our capacity to predict the future of OM storage in soils.

5. Conclusions

Building upon the theoretical framework of Schmidt et al. (2011), this study investigated ecosystem-scale controls on soil OM dynamics in a wide range of soils co-occurring in a restricted geographical area of the Swiss Alps. We used OM thermal stability as a proxy for OM dynamics, broadly understood as processes leading to patterns of OM distribution and properties. The study of the whole soil profile allowed to show a radical shift in the nature of predictors of OM dynamics between soil layers. In the litter layer, the OM thermal stability was related to its composition (a product of the initial composition of plant inputs and probably more importantly, their degree of microbial processing), suggesting a dominant biological and biochemical control. In the topsoil, OM thermal stability was mainly related to the OM content, which represented the balance between factors influencing inputs (litter in-mixing, fine root density) and outputs (waterlogging). In the subsoil, geochemical and pedogenetic parameters rose to the forefront as predictors of OM thermal stability. These results suggest that soil horizons act as interacting yet distinct functional units in terms of OM dynamics and are likely to respond differently to external forcing. Therefore, next-generation conceptual or numerical models of soil OM cycling would be greatly improved by the implementation of depth-resolved schemes. Moreover, multi-disciplinary approaches, as the present one, may prove to be particularly relevant for the understanding and the prediction of soil OM fate under fast climate change.

Contribution statement

M.M. and P.V. designed the sampling strategy, performed vegetation records and soil descriptions in the field. M.M. analysed soil samples. M.M., S.G., and D.S. analysed data. P.V. and E.P.V. supervised the work. E.P.V. funded the work and contributed to design the sampling strategy. All co-authors contributed to the writing and the interpretation of data.

Acknowledgments

We thank Marie-José Petétot for her help in plant inventories and soil descriptions of the Morteys site, and analysis of the relative soil samples. We thank also Loïc Liberati, Swanee Messerli, Jessica Rion, Aurélie Rubin, Ayumi Koishi, Yohan Ancey and Jérémy Tritz for their help in the field, pH measurements and sample preparations. Dr. Thierry Adatte (ISTE, University of Lausanne) performed Rock-Eval and CHNS analyses. We are very grateful to Aline Buri for her suggestions on statistical analyses. The “Fondation Herbette” kindly supported Dr. David Sebag during his stays at the University of Lausanne.

Appendix A. Supplementary data

Supplementary data to this article can be found online at https://doi.org/10.1016/j.geoderma.2018.05.011.

References

Aber, J.D., Melillo, J.M., 1982. Nitrogen immobilization in decaying hardwood leaf litter as a function of initial nitrogen and lignin content. Can. J. Bot. 60, 2263–2269.
Aber, J.D., Melillo, J.M., Mcclaugherty, C.A., 1990. Predicting long-term patterns of mass-loss, nitrogen dynamics, and soil organic-matter formation from initial fine litter chemistry in temperate forest ecosystems. Can. J. Bot. 68, 2201–2208.
Adhikari, K., Hartemink, A.E., 2016. Linking soils to ecosystem services - a global review. Geoderma 262, 101–111.
Anderson, D.R., Burnham, K.P., Thompson, W.L., 2000;al.,. Null hypothesis testing: problems, prevalence, and an alternative. J. Wildl. Manag. 64, 912–923.
Baize, D., Girard, M.-C., 2009. Référentiel pédologique. Association française pour l'étude du sol (AFES), Versailles Cedex.
Baptist, F., Yoccoz, N.G., Choler, P., 2010. Direct and indirect control by snow cover over decomposition in alpine tundra along a snowmelt gradient. Plant Soil 328, 397–410.
Barré, P., Plante, A.F., Cécillon, L., Lutfalla, S., Baudin, F., Bernard, S., et al., 2016. The energetic and chemical signatures of persistent soil organic matter. Biogeochemistry 130, 1–12.
Baruck, J., Nestroy, O., Sartori, G., Baize, D., Traidl, R., Vrščaj, B., et al., 2016. Soil classification and mapping in the Alps: the current state and future challenges. Geoderma 264, 312–331.
Batjes, N.H., 1996. Total carbon and nitrogen in the soils of the world. Eur. J. Soil Sci. 47, 151–163.
Burnham, K.P., Anderson, D.R., 2002. Model selection and multimodel inference. In: A Practical Information-Theoretic Approach, 2nd ed. Springer, New York.
Carrie, J., Sanei, H., Stern, G., 2012. Standardisation of Rock-Eval pyrolysis for the analysis of recent sediments and soils. Org. Geochem. 46, 38–53.
Davidson, E.A., Janssens, I.A., 2006. Temperature sensitivity of soil carbon decomposition and feedbacks to climate change. Nature 440, 165–173.
Delarze, R., Gonseth, Y., Eggenberg, S., Vust, M., 2015. Guide des milieux naturels de Suisse, 3rd ed. Rossolis, Bussigny.
Derrien, D., Marol, C., Balabane, M., Balesdent, J., 2006. The turnover of carbohydrate carbon in a cultivated soil estimated by C-13 natural abundances. Eur. J. Soil Sci. 57, 547–557.
Diochon, A., Gillespie, A.W., Ellert, B.H., Janzen, H.H., Gregorich, E.G., 2016. Recovery and dynamics of decomposing plant residue in soil: an evaluation and three fractionation methods. Eur. J. Soil Sci. 67, 196–205.
FAO, 2006. Guidelines for soil description, 4th ed. Food and Agriculture Organization of the United Nations (FAO), Rome, Italy.
Favilli, F., Cherubini, P., Collenberg, M., Egli, M., Sartori, G., Schoch, W., Haeberli, W., 2010. Charcoal fragments of Alpine soils as an indicator of landscape evolution during the Holocene in Val di Sole (Trentino, Italy). The Holocene 20, 67–79.

Fierer, N., Allen, A.S., Schimel, J.P., Holden, P.A., 2003. Controls on microbial CO_2 production: a comparison of surface and subsurface soil horizons. Glob. Chang. Biol. 9, 1322–1332.
Gelman, A., 2008. Scaling regression inputs by dividing by two standard deviations. Stat. Med. 27, 2865–2873.
Gleixner, G., Bol, R., Balesdent, J., 1999. Molecular insight into soil carbon turnover. Rapid Commun. Mass Spectrom. 13, 1278–1283.
Gleixner, G., Poirier, N., Bol, R., Balesdent, J., 2002. Molecular dynamics of organic matter in a cultivated soil. Org. Geochem. 33, 357–366.
Grand, S., Lavkulich, L.M., 2012. Effect of forest harvest on soil carbon and related variables in Canadian Spodosols. Soil Sci. Soc. Am. J. 76, 1816–1827.
Grand, S., Rubin, A., Verrecchia, E.P., Vittoz, P., 2016. Variation in soil respiration across soil and vegetation types in an Alpine valley. PLoS One 11, e0163968.
Gregorich, E.G., Gillespie, A.W., Beare, M.H., Curtin, D., Sanei, H., Yanni, S.F., 2015. Evaluating biodegradability of soil organic matter by its thermal stability and chemical composition. Soil Biol. Biochem. 91, 182–191.
Harrell, F.E., 2001. Regression Modeling Strategies: With Applications to Linear Models, Logistic Regression, and Survival Analysis. Springer, New York.
Heim, A., Schmidt, M.W.I., 2007. Lignin turnover in arable soil and grassland analysed with two different labelling approaches. Eur. J. Soil Sci. 58, 599–608.
Hobbie, S.E., Chapin, F.S., 1996. Winter regulation of tundra litter carbon and nitrogen dynamics. Biogeochemistry 35, 327–338.
IUSS Working Group, 2015. World reference base for soil resources 2014, update 2015. International soil classification system for naming soils and creating legends for soil maps. In: World Soil Resources Reports No. 106. FAO, Rome.
Ivy-Ochs, S., Schafer, J., Kubik, P.W., Synal, H.A., Schluchter, C., 2004. Timing of deglaciation on the northern Alpine foreland (Switzerland). Eclogae Geol. Helv. 97, 47–55.
Jabiol, B., Zanella, A., Ponge, J.-F., Sartori, G., Englisch, M., Delft, B., et al., 2013. A proposal for including humus forms in the World Reference Base for Soil Resources (WRB-FAO). Geoderma 192, 286–294.
Jobbagy, E.G., Jackson, R.B., 2000. The vertical distribution of soil organic carbon and its relation to climate and vegetation. Ecol. Appl. 10, 423–436.
Knutson, E.O., Sood, S.K., Stockham, J.D., 1976. Aerosol collection by snow and ice crystals. Atmos. Environ. 10, 395–402.
Kögel-Knabner, I., Guggenberger, G., Kleber, M., Kandeler, E., Kalbitz, K., Scheu, S., et al., 2008. Organo-mineral associations in temperate soils: integrating biology, mineralogy, and organic matter chemistry. J. Plant Nutr. Soil Sci. 171, 61–82.
Lafargue, E., Marquis, F., Pillot, D., 1998. Rock-Eval 6 applications in hydrocarbon exploration, production, and soil contamination studies. Rev. Inst. Fr. Pétrol. 53, 421–437.
Landolt, E., Bäumler, B., Erhardt, A., Hegg, O., Klötzli, F.A., Lämmler, W., et al., 2010. Flora Indicativa. Ecological Indicator Values and Biological Attributes of the Flora of Switzerland and the Alps. Haupt, Bern, Switzerland.
Legendre, P., Gallagher, E.D., 2001. Ecologically meaningful transformations for ordination of species data. Oecologia 129, 271–280.
Lehmann, J., Kleber, M., 2015. The contentious nature of soil organic matter. Nature 528, 60–68.
Leifeld, J., Zimmermann, M., Fuhrer, J., Conen, F., 2009. Storage and turnover of carbon in grassland soils along an elevation gradient in the Swiss Alps. Glob. Chang. Biol. 15, 668–679.
Manzoni, S., Jackson, R.B., Trofymow, J.A., Porporato, A., 2008. The global stoichiometry of litter nitrogen mineralization. Science 321, 684–686.
Marschner, B., Brodowski, S., Dreves, A., Gleixner, G., Gude, A., Grootes, P.M., et al., 2008. How relevant is recalcitrance for the stabilization of organic matter in soils? J. Plant Nutr. Soil Sci. 171, 91–110.
Melillo, J.M., Aber, J.D., Muratore, J.F., 1982. Nitrogen and lignin control of hardwood leaf litter decomposition dynamics. Ecology 63, 621–626.
Mullen, R.B., Schmidt, S.K., Jaeger, C.H., 1998. Nitrogen uptake during snowmelt by the snow buttercup, *Ranunculus adoneus*. Arct. Alp. Res. 30, 121–125.
Oberhänsli, R., Schenker, F., Mercolli, I., 1988. Indications of Variscan nappe tectonics in the Aar Massif. Schweiz. Mineral. Petrogr. Mitt. 68, 509–520.
Plante, A.F., Fernandez, J.M., Haddix, M.L., Steinweg, J.M., Conant, R.T., 2011. Biological, chemical and thermal indices of soil organic matter stability in four grassland soils. Soil Biol. Biochem. 43, 1051–1058.
Ponge, J.F., Chevalier, R., Loussot, P., 2002. Humus index: an integrated tool for the assessment of forest floor and topsoil properties. Soil Sci. Soc. Am. J. 66, 1996–2001.
Preston, C.M., Nault, J.R., Trofymow, J.A., Smyth, C., Grp, C.W., 2009. Chemical changes during 6 years of decomposition of 11 litters in some Canadian forest sites. Part 1. Elemental composition, tannins, phenolics, and proximate fractions. Ecosystems 12, 1053–1077.
Rasmussen, C., Heckman, K., Wieder, W.R., Keiluweit, M., Lawrence, C.R., Behre, A.A., et al., 2018. Beyond clay: towards an improved set of variables for predicting soil organic matter content. Biogeochemistry 137, 297–306.
Rowley, M., Grand, S., Verrecchia, E., 2018. Calcium-mediated stabilisation of soil organic carbon. Biogeochemistry 137, 27–49.
Rumpel, C., Kögel-Knabner, I., 2011. Deep soil organic matter-a key but poorly understood component of terrestrial C cycle. Plant Soil 338, 143–158.
Rumpel, C., Kögel-Knabner, I., Bruhn, F., 2002. Vertical distribution, age, and chemical composition of organic, carbon in two forest soils of different pedogenesis. Org. Geochem. 33, 1131–1142.
Rumpel, C., Eusterhues, K., Kögel-Knabner, I., 2004. Location and chemical composition of stabilized organic carbon in topsoil and subsoil horizons of two acid forest soils. Soil Biol. Biochem. 36, 177–190.
Saenger, A., Cecillon, L., Sebag, D., Brun, J.J., 2013. Soil organic carbon quantity, chemistry and thermal stability in a mountainous landscape: a Rock-Eval pyrolysis survey. Org. Geochem. 54, 101–114.
Saenger, A., Cecillon, L., Poulenard, J., Bureau, F., De Danieli, S., Gonzalez, J.M., Brun, J.J., 2015. Surveying the carbon pools of mountain soils: a comparison of physical fractionation and Rock-Eval pyrolysis. Geoderma 241, 279–288.
Salomé, C., Nunan, N., Pouteau, V., Lerch, T.Z., Chenu, C., 2010. Carbon dynamics in topsoil and in subsoil may be controlled by different regulatory mechanisms. Glob. Chang. Biol. 16, 416–426.
Schiedung, M., Don, A., Wordell-Dietrich, P., Alcántara, V., Kuner, P., Guggenberger, G., 2017. Thermal oxidation does not fractionate soil organic carbon with differing biological stabilities. J. Plant Nutr. Soil Sci. 180, 18–26.
Schimel, D.S., 1995. Terrestrial ecosystems and the carbon-cycle. Glob. Chang. Biol. 1, 77–91.
Schimel, J.P., Schaeffer, S.M., 2012. Microbial control over carbon cycling in soil. Front. Microbiol. http://dx.doi.org/10.3389/fmicb.2012.00348.
Schimel, J.P., Weintraub, M.N., 2003. The implications of exoenzyme activity on microbial carbon and nitrogen limitation in soil: a theoretical model. Soil Biol. Biochem. 35, 549–563.
Schlesinger, W.H., Bernhardt, E.S., 2013. Biogeochemistry: An Analysis of Global Change, 3rd ed. Elsevier/Academic Press.
Schmidt, M.W.I., Torn, M.S., Abiven, S., Dittmar, T., Guggenberger, G., Janssens, I.A., et al., 2011. Persistence of soil organic matter as an ecosystem property. Nature 478, 49–56.
Sebag, D., Disnar, J.R., Guillet, B., Di Giovanni, C., Verrecchia, E.P., Durand, A., 2006. Monitoring organic matter dynamics in soil profiles by 'Rock-Eval pyrolysis': bulk characterization and quantification of degradation. Eur. J. Soil Sci. 57, 344–355.
Sebag, D., Verrecchia, E.P., Cécillon, L., Adatte, T., Albrecht, R., Aubert, M., et al., 2016. Dynamics of soil organic matter based on new Rock-Eval indices. Geoderma 284, 185–203.
Six, J., Conant, R.T., Paul, E.A., Paustian, K., 2002. Stabilization mechanisms of soil organic matter: implications for C-saturation of soils. Plant Soil 241, 155–176.
Sollins, P., Homann, P., Caldwell, B.A., 1996. Stabilization and destabilization of soil organic matter: mechanisms and controls. Geoderma 74, 65–105.
Soucémarianadin, L., Cécillon, L., Chenu, C., Baudin, F., Nicolas, M., Girardin, C., Barré, P., 2018a. Is Rock-Eval 6 thermal analysis a good indicator of soil organic carbon lability? A method-comparison study in forest soils. Soil Biol. Biochem. 117, 108–116.
Soucémarianadin, L.N., Cécillon, L., Guenet, B., Chenu, C., Baudin, F., Nicolas, M., et al., 2018b. Environmental factors controlling soil organic carbon stability in French forest soils. Plant Soil. http://dx.doi.org/10.1007/s11104-018-3613-x.
Spielvogel, S., Prietzel, J., Kögel-Knabner, I., 2008. Soil organic matter stabilization in acidic forest soils is preferential and soil type-specific. Eur. J. Soil Sci. 59, 674–692.
Symonds, M.R.E., Moussall, I.A., 2011. A brief guide to model selection, multimodel inference and model averaging in behavioural ecology using Akaike's information criterion. Behav. Ecol. Sociobiol. 65, 13–21.
Theurillat, J.P., Felber, F., Geissler, P., Gobat, J.-M., Fierz, M., Fischlin, A., et al., 1998. Sensitivity of plant and soil ecosystems of the Alps to climate change. In: Cebon, P., Davies, H.C., Imboden, D., Jaeger, C.C. (Eds.), Views From the Alps. MIT Press, Massachusetts, pp. 225–308.
van der Voort, T.S., Hagedorn, F., McIntyre, C., Zell, C., Walthert, L., Schleppi, P., et al., 2016. Variability in C-14 contents of soil organic matter at the plot and regional scale across climatic and geologic gradients. Biogeosciences 13, 3427–3439.
Vinduskova, O., Sebag, D., Cailleau, G., Brus, J., Frouz, J., 2015. Methodological comparison for quantitative analysis of fossil and recently derived carbon in mine soils with high content of aliphatic kerogen. Org. Geochem. 89-90, 14–22.
von Lützow, M., Kögel-Knabner, I., Ekschmitt, K., Matzner, E., Guggenberger, G., Marschner, B., Flessa, H., 2006. Stabilization of organic matter in temperate soils: mechanisms and their relevance under different soil conditions - a review. Eur. J. Soil Sci. 57, 426–445.
von Lützow, M., Kögel-Knabner, I., Ludwig, B., Matzner, E., Flessa, H., Ekschmitt, K., et al., 2008. Stabilization mechanisms of organic matter in four temperate soils: development and application of a conceptual model. J. Plant Nutr. Soil Sci. 171, 111–124.
Vonlanthen, C.M., Bühler, A., Veit, H., Kammer, P.M., Eugster, W., 2006. Alpine plant communities: a statistical assessment of their relation to microclimatological, pedological, geomorphological, and other factors. Phys. Geogr. 27, 137–154.
Webster, R., 2007. Analysis of variance, inference, multiple comparisons and sampling effects in soil research. Eur. J. Soil Sci. 58, 74–82.
Woolgrove, C.E., Woodin, S.J., 1996. Ecophysiology of a snow-bed bryophyte *Kiaeria starkei* during snowmelt and uptake of nitrate from meltwater. Can. J. Bot. 74, 1095–1103.
Zimmermann, N.E., Kienast, F., 1999. Predictive mapping of alpine grasslands in Switzerland: species versus community approach. J. Veg. Sci. 10, 469–482.